23rd ABCM International Congress of Mechanical Engineering
December 6-11, 2015, Rio de Janeiro, RJ, Brazil

NUMERICAL STUDY AND VALIDATION OF NON-NEWTONIAN FLUID HAMMER IN CIRCULAR PIPES

Tainan Gabardo Miranda dos Santos
Gabriel Merhy de Oliveira
Cezar Otaviano Ribeiro Negrão
Federal University of Technology – Paraná – Av. Sete de Setembro, 3165, Curitiba – PR, CEP 80230-901
tainan@alunos.utfpr.edu.br
gabrielm@utfpr.edu.br
negrao@utfpr.edu.br

Abstract. *This study investigates the water hammer theory on non-Newtonian fluids through numerical simulation. The effect of sudden valve closure on the flow dynamics of Power-Law fluids in circular pipes is studied. The model is one-dimensional, but the local velocity is radius dependent. The flow is laminar, weakly compressible and isothermal. The mass conservation, momentum balance, state and constitutive equation are iteratively solved using the finite volumes method. First order Upwind Scheme is used to approximate nonlinear terms. Implicit Time Integration is used to approximate temporal terms. Present results are compared to the experimental data of Holmboe and Rouleau (1967) and to the Power-Law results of the model of Wahba (2013). Those comparisons show good agreement and demonstrate the importance of shear-thinning and shear-thickening in transient behavior. The proposed model represents well the attenuation verified experimentally. It also presents a new solution methodology in which different fluids can be easily changed through a constitutive equation.*

Keywords: *Unsteady pipe flow, Power law model, Fluid transients*

1. INTRODUCTION

Fluid hammer is defined by Watters (1984) as transient flows generated in pipelines as a results of sudden changes in flow conditions. These changes may be occasioned by the rapid closure of a valve or the shutdown of the pump. Holmboe and Rouleau (1967) conducted an experiment with water and oil in which the inlet of the pipeline is pressured by an infinite reservoir and the outlet valve is suddenly closed. This work and the one of Wylie *et al*. (1993) pointed out that models that do not consider the dependency of the friction factor with oscillation frequencies are less dissipative than experimental tests. Wahba (2008) and Wahba (2013) proposed a two-dimensional model that was capable of representing the viscous dissipation for the oil in the experiment of Holmboe and Rouleau (1967).

A similar problem occurs during drilling operations when some valves are opened by pressure difference. Drilling fluids are pumped into the drillpipe and the pressure is transmitted to the bottom of the well. As the pressure level is high enough, the valve is then opened. Oliveira *et al.* (2012) reported that in some cases only a fraction of the inlet pressure reaches the outlet of the pipeline. So the valve remains closed. For the purpose of solving this problem sometimes it is necessary to remove the drilling fluid and replace it for water, but this operation is slow and expensive.

As the mechanisms of pressure transmission, restart of the flow and fluid hammer are not yet well understood, more studies are necessary to comprehend those phenomenons. Many works on oil and drilling fluids, such as: Davidson *et al.* (2004), Vinay *et al.* (2006 e 2007) e Wachs *et al.* (2009), studied the flow start up, a problem in which the outlet is opened. The works of Oliveira *et al.* (2010) and Negrão *et al.* (2011) tried to understand this phenomenon by utilizing a one-dimensional model that adopts the hypothesis that the shear stress is linearly dependent of the radius.

Oliveira *et al.* (2015) proposed a one-dimensional mathematical model to simulate viscoplastic fluid hammer in which the fluid is assumed to behave as a Bingham plastic. The authors compared their results with those from the experiment of Holmboe and Rouleau (1967) for oil. As they adopted the hypothesis that the shear stress is radius dependent, their results underestimate the attenuation of the peaks of pressure.

In order to comprehend this phenomenon, the present work proposes a mathematical model for the fluid hammer in circular pipes relaxing the hypothesis of Oliveira *et al.* (2015) that the shear stress is linearly dependent of the radius. This paper proposes a new solution methodology in which new Non Newtonian fluids may be included through a constitutive equation. The model is validated by comparing results with the experimental data of Holmboe and Rouleau (1967) for water and oil. It also compares with the numerical data of Wahba (2013) for Power Law fluids. Finally, the shear-thinning and shear-thickening effects are evaluated along the axial direction for different times.

2. MATHEMATICAL MODEL

2.1 Problem description

The fluid hammer problem is represented by a horizontal pipeline of length L and of diameter D filled with fluid flowing at the steady state and a rapid closure valve at the outlet. Figure 1 illustrates the geometry of the problem. The fluid is maintained at constant pressure and suddenly the valve at outlet is closed.

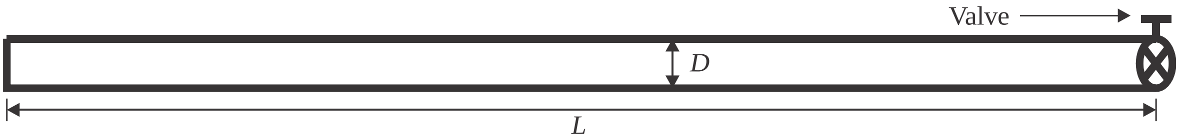

Figure 1. Geometry of the problem

The tube walls are rigid, so there is no deformation in the structure. The following assumptions are used to model this problem: the flow is one-dimensional, laminar, weakly compressible and isothermal; the local velocity is dependent of the radius; the pressure and the fluid density are axial dependent, the pipeline is horizontal; and the shear stress is calculated by using a constitutive equation.

2.2 Governing Equations

By considering the assumptions above, the mass conservation and momentum balance equations are then written as:

$$\frac{\partial \rho}{\partial t}+\frac{\partial}{\partial z}\ \rho V\ =0 \tag{1}$$

$$\frac{\partial}{\partial t}\ \rho u\ +\frac{\partial}{\partial z}\ \rho u u\ =\frac{\partial P}{\partial z}-\frac{1}{r}\frac{\partial}{\partial r}\ r\tau \tag{2}$$

where ρ is the fluid density, V is the average axial velocity, u is the local velocity, P is the pressure, τ is the shear stress, r, z and t are, respectively, the radial, axial and temporal coordinates. The isothermal compressibility, α, is defined as (Anderson, 1990):

$$\alpha=\frac{1}{\rho}\left(\frac{\partial \rho}{\partial P}\right)_T=\frac{1}{\rho c^2} \tag{3}$$

where T is the temperature and c is the wave speed. By integrating Eq. 3 from the reference to the current condition, a relation between fluid density and pressure, called state equation, is obtained:

$$P=P_0+\frac{1}{\alpha}\ln\left(\frac{\rho}{\rho_0}\right) \tag{4}$$

where the 0 index is the reference condition.

2.3 Constitutive Equation

Generically, the constitutive equation is represented as:

$$\tau=\eta\dot{\gamma}=\eta\frac{\partial u}{\partial r} \tag{5}$$

where η is the shear viscosity and $\dot{\gamma}$ is the shear rate.

The fluids used in the experimental rig of Holmboe and Rouleau (1967) are water and oil, both Newtonian fluids. But the comparison with Wahba (2013) utilizes a Power Law fluid. So the dynamic viscosity for the Newtonian fluid is constant (Bird, 1987):

$$\eta_{Newtonian} = \mu \tag{6}$$

where μ is the shear viscosity. On the other hand, the shear viscosity for the Power Law fluid is shear rate dependent and it is given by (Bird, 1987):

$$\eta_{Power\ Law} = k\dot{\gamma}^{n-1} = k\left(\frac{\partial u}{\partial r}\right)^{n-1} \tag{7}$$

where k is the consistency index and n is the Power Law index.

3. SOLUTION ALGORITHM

The mathematical model is solved by using the finite volume method and the nonlinear terms are discretized with the Upwind scheme (Patankar, 1980). The fully implicit method is used in temporal approximation. The mass conservation and state equations are discretized with one-dimensional grids divided axially in NZ control volumes. The constitutive equation uses one-dimensional meshes divided in NR cells. The mesh of the momentum balance equation is two-dimensional with control volumes of an area of Δz by Δr.

In the axial direction, pressure and fluid density grids are displaced in relation to average axial velocity grid. Pressure and fluid density are evaluated at the center of each volume and average velocity at the borders. In the radial direction, local velocity grid is displaced of shear stress mesh. Local velocity is evaluated at the center and shear stress at the borders of each cell. As pressure and fluid density are only axial dependent, their position is represented by the lowercase index i, while average axial velocity is indicated by uppercase I. Local velocity is represented by the indexes I and j (radial), whereas shear stress are evaluated in I and J. The indexes k and $k+1$ indicate the current and future instants.

Thereby the discretized mass conservation equation is represented by:

$$\rho_i^{k+1} = \frac{b_i\rho_i^k + c_i}{a_i} \tag{8}$$

where

$$a_i = V_{I+1}^{k+1} + \frac{\Delta z}{\Delta t},\ b_i = \frac{\Delta z}{\Delta t},\ c_i = V_I^{k+1} \tag{9}$$

The discretized state equation:

$$P_i^{k+1} = P_0 + \frac{1}{\alpha}\ln\left(\frac{\rho_i^{k+1}}{\rho_0}\right) \tag{10}$$

The discretized momentum balance equation:

$$u_{I,j}^{k+1} = \frac{B_{I,j}u_{I,j}^k + C_{I,j}u_{I-1,j}^{k+1} + D_{I,j}\tau_{I,\mathrm{J}}^{k+1} + E_{I,j}\tau_{I,\mathrm{J}-1}^{k+1} + F_{I,j}}{A_{I,j}} \tag{11}$$

where

$$A_{I,j} = \frac{\rho_i^{k+1} + \rho_{i-1}^{k+1}}{2}\frac{\Delta z}{\Delta t} + \rho_i^{k+1}\frac{u_{I+1,j}^{k+1} + \rho_{I,j}^{k+1}}{2},\ B_{I,j} = \frac{\rho_i^k + \rho_{i-1}^k}{2}\frac{\Delta z}{\Delta t},\ C_{I,j} = \rho_{i-1}^{k+1}\frac{u_{I,j}^{k+1} + \rho_{I-1,j}^{k+1}}{2} \tag{12}$$

$$D_{I,j} = -\frac{r_J}{r_j}\frac{\Delta z}{\Delta r},\ E_{I,j} = -\frac{r_{J-1}}{r_j}\frac{\Delta z}{\Delta r},\ F_{I,j} = -\ P_i^{k+1} - P_{i-1}^{k+1} + \frac{\rho_i^{k+1} + \rho_{i-1}^{k+1}}{2}g\Delta z \tag{13}$$

The discretized constitutive equation:

$$\tau_{I,J}^{k+1} = \eta_{I,J}^{k+1} \frac{u_{I,\mathrm{j}+1}^{k+1} - u_{I,\mathrm{j}}^{k+1}}{\Delta r} \tag{14}$$

where

$$\eta_{I,J,Newtonian}^{k+1} = \mu \tag{15}$$

$$\eta_{I,J,\text{Power Law}}^{k+1} = \mu \left(\frac{u_{I,\mathrm{j}+1}^{k+1} - u_{I,\mathrm{j}}^{k+1}}{\Delta r} \right)^{n-1} \tag{16}$$

The algorithm to solve this set of equations is: (i) the data is read and the variables are initialized; (ii) the average velocity is calculated for each axial section; (iii) the coefficients of the mass conservation equation are calculated; (iv) the fluid density is determined for each axial position; (v) the pressure is determined by the state equation; (vi) the coefficients of the constitutive equation are calculated; (vii) the shear stress is determined for each set of axial and radial position; (viii) the coefficients of the momentum balance equation are calculated; (ix) the local velocity is determined for each set of axial and radial position; (x) the convergence criterion is verified; and (xi) the maximal simulation time, $t_{\max}$, is verified.

The convergence criterion, $\varepsilon_{\max}$, is obtained by the residue of the mass conservation equation:

$$\varepsilon_{\max} = \frac{1}{\rho_{in} V_{in}} \sum_i \; \rho_i^{k+1} a_i - \rho_i^k b_i - c_i \tag{17}$$

where the index in represents the initial value.

In order to assure that the results are not grid and residue dependent, an analysis of grid sensibility was conducted. It was verified that a mesh of 2000 axial and 40 radial cells with a maximal residue of 0.001 is sufficient for an independent result. Besides Fortuna (2000) said that it is necessary to verify a stability criterion (CFL, Equation 24), because low CFL values may cause instability and numerical dispersions. Therefore, a CFL = 1 was chosen for the simulations.

$$CFL = c \frac{\Delta t}{\Delta z} \leq 1 \tag{18}$$

4. EXPERIMENTAL RIG

The experimental rig to generate the fluid hammer of Holmboe and Rouleau (1967) is shown in Fig. 2. A rapid closing valve was mounted at the end of a copper pipeline with 36.09 m of length and 25.4 mm of diameter. The valve used a sliding spool that actuated by the impact of a mass accelerated by compressed air. The pipeline was involved by concrete to reduce vibrations. A 60 gallons tank, which was maintained at constant pressure due to compressed air, represented an infinite reservoir at the inlet of the pipe. Two Norwood transducers were positioned at the middle (B, 18.045 m) and at the outlet (A, 36.09 m) of the pipeline. The results were amplified by Honeywell carrier amplifiers and recorded by a Honeywell "Viscorder".

The test sequence was: (i) the valve was opened for the fluid to flow until steady state was reached; (ii) the valve at outlet of the pipeline was suddenly closed; (iii) the pressure was maintained constant; and (iv) the pressure was recorded until the fluid stopped.

Initially the fluid is flowing through the pipeline with constant velocity, $V\;z,t=0\;=V_{in}$, and the pressure is axially distributed as the analytical solution for a power law fluid at equilibrium. Then the valve at the outlet is closed, therefore the outlet velocity is zero, $u\;r,z=L_T,t\;=0$ and $V\;r,z=L_T,t\;=0$. The inlet pressure remains constant, $P\;z=0,t\;=P_{in}$.

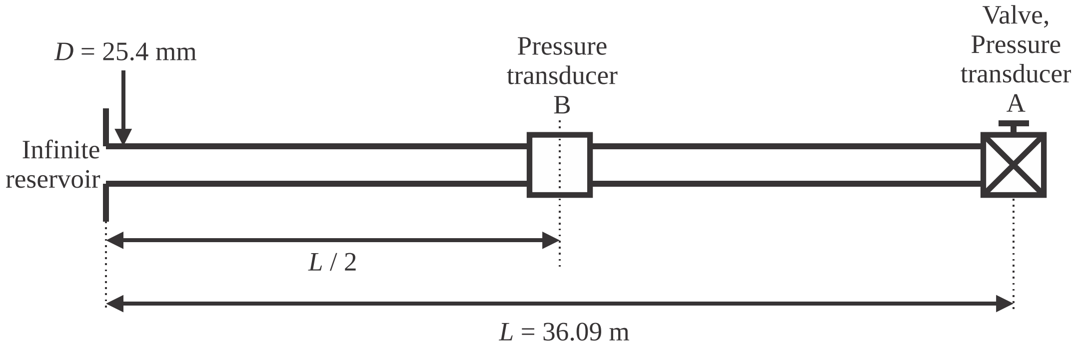

Figure 2. Schematic diagram of Holmboe and Rouleau (1967) water hammer experiment

5. MODEL VALIDATION

In fluid hammer problems, it is usual to display results as a function of the pressure head. In this work non-dimensional head pressure and time are going to be used:

$$h^* = \frac{P - P_{in}}{\rho a V_{in}} \tag{19}$$

$$t^* = \frac{at}{L} \tag{20}$$

5.1 Experimental data of Holmboe and Rouleau (1967)

In order to evaluate their model, Holmboe and Rouleau (1967) tested two fluids: water and oil. The proprieties of those fluids are shown in Tab. 1. They were obtained from, respectively, White (2003) and Wahba (2013).

Table 1. Water and oil properties for fluid hammer experiment of Holmboe and Rouleau (1967).

Properties	Water	Oil
ρ_0 (kg/m³)	997	876
μ (Pa.s)	0.00086	0.03484
c (m/s)	1465	1324

For the water test, the initial average velocity was 0.244 m/s and the initial pressure was 375.6 Pa. Figure 3(a) illustrates the results for the pressure transducer A, which is located at the outlet. One can note that the pressure head suddenly rises at $t^* = 0$ due to the closure of the valve. One can observe that both frequency and amplitude show good agreement between experimental and numerical data. The quadratic shape of the cycles indicates low dissipation and energy loss.

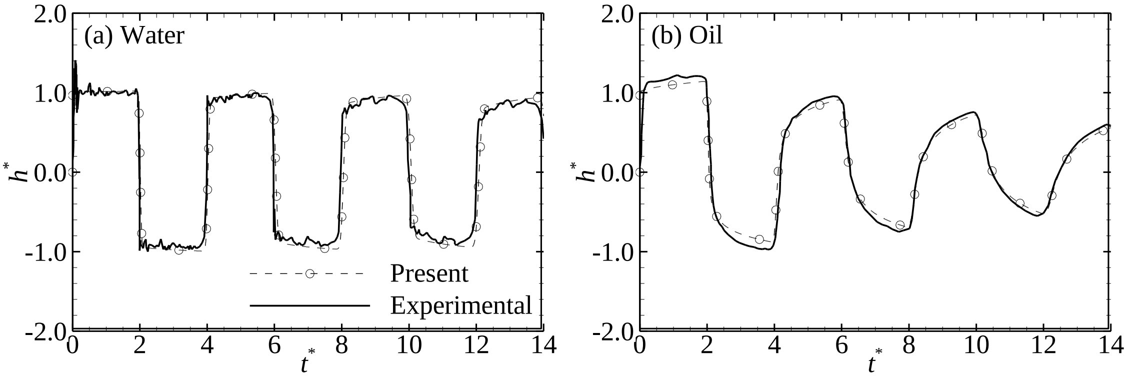

Figure 3. Pressure head evolution in time at the valve (outlet) for experimental data of Holmboe and Rouleau (1967) and for numerical data calculated by the present model for: (a) water and (b) oil

In order to present the viscous effect, Holmboe and Rouleau (1967) selected an oil with cinematic viscosity of 1.3×10^{-3} m/s^2 at 80 ºF (50 times the cinematic viscosity of the water). The inlet average velocity and pressure were, respectively, 0.128 m/s and 7983 Pa, that represents a fluid with Reynold's number of 82. The results for pressure transducer A are presented in Fig. 3(b). One can note that the curve shape is more damped, each cycle is more dissipative, maximum and minimum values decrease a lot faster than for the water. Once again numerical data shows good agreement with experimental and the period of oscillation is well represented. But, the amplitude of oscillation has a maximum difference of 10%.

5.2 Numerical data of Wahba (2013)

Wahba (2013) conducted a numerical analysis of power law fluids during a fluid hammer. So the procedures are the same as described for the experiment rig of Holmboe and Rouleau (1967). In order to compare results, a constant Reynold's number of 82 was used. Table 2 presents the values for initial inlet average velocity and pressure for each power law index. The consistency index is k = 0.03484 Pa.s^n. Figure 4 compares the numerical data of the present model and of the model of Wahba (2013) by showing the evolution of pressure head in time on pressure transducer A for n = 0.6, 0.8, 1.2 and 1.4. One can note that both models show remarkable agreement. It is also important to observe that the greater the power law index, the fastest the pressure head dissipates.

Table 2. Initial inlet pressure and average velocity for different power law indexes.

n	V_{in} (m/s)	P_{in} (Pa)
0.6	0.048	1136.3
0.8	0.073	2624.8
1.2	0.311	47756.4
1.4	1.321	860567.3

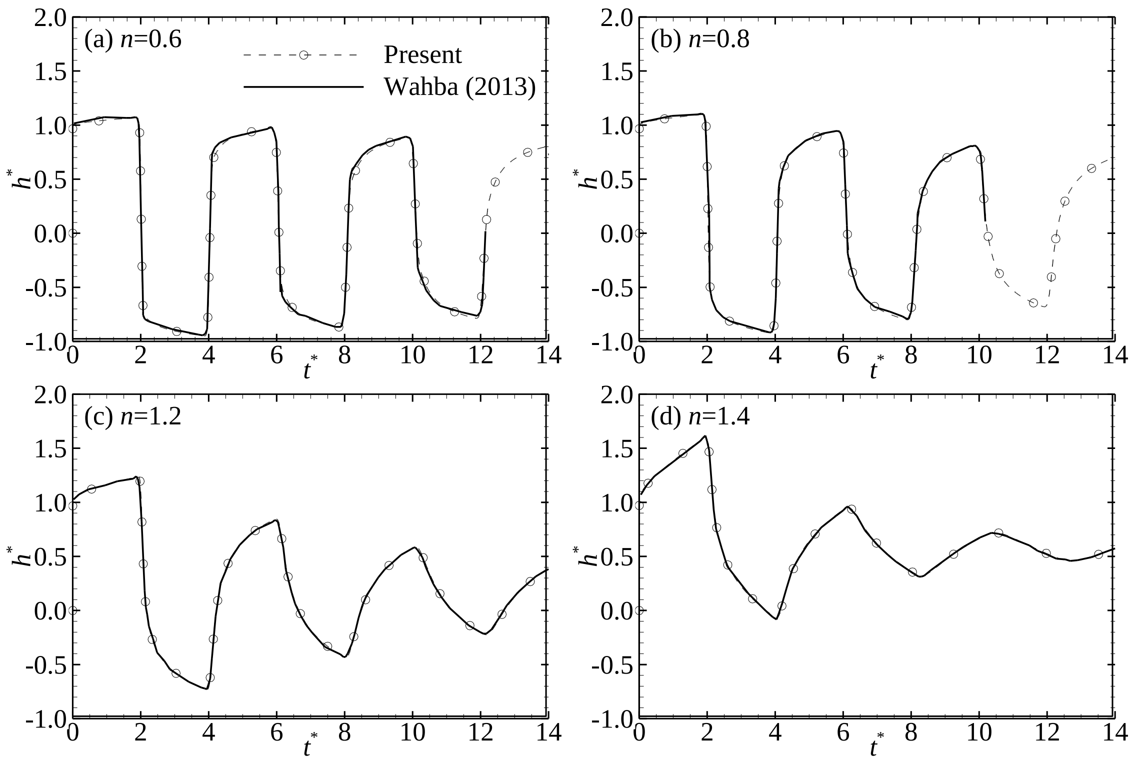

Figure 4. Pressure head at the valve (outlet) for different power indexes: (a) 0.6, (b) 0.8, (c) 1.2 and (d) 1.4

Figure 5 shows the pressure along the axial direction for eight non dimensional times: 1, 2, 3, 5, 6 and 100. One can note that the greater the power law index the faster the pressure head is distributed. So shear thickening fluids ($n > 1$) have a faster attenuation of the pressure. On the other side, shear thinning fluids ($n < 1$) take more time to reach the equilibrium. Figure 5(e) shows the steady state. One can observe that in order to obtain the same Reynold's number, the steady state pressure head for shear thickening fluids changes axially more than for shear thinning fluids.

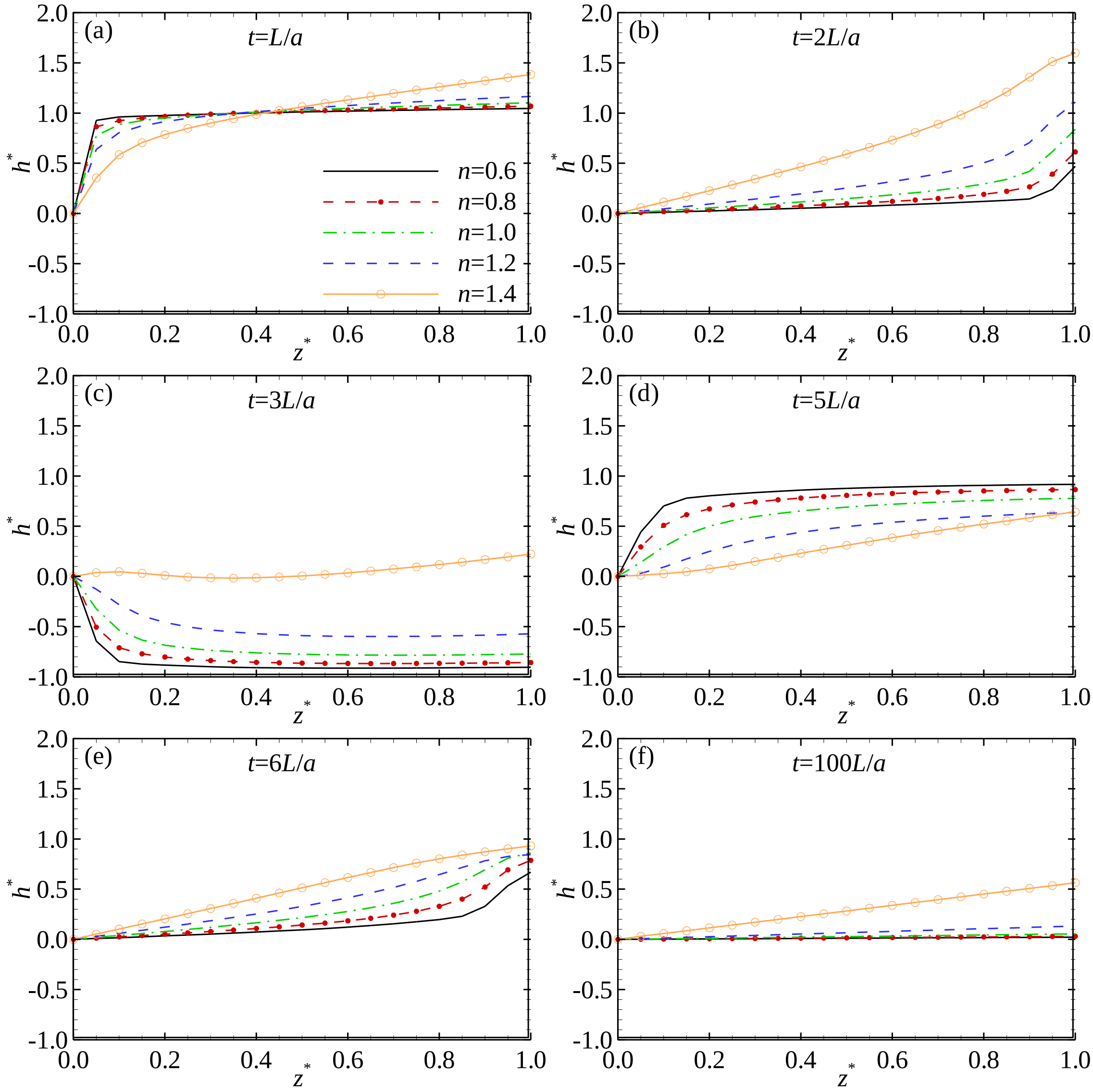

Figure 5. Pressure head profile for non-dimensional times of: (a) $t^* = L/a$, (b) $t^* = 2L/a$, (c) $t^* = 3L/a$, (d) $t^* = 5L/a$, (e) $t^* = 7L/a$, and (f) $t^* = 100L/a$

6. CONCLUSION

This work presented a mathematical model to simulate the fluid hammer phenomenon of Newtonian and Non-Newtonian fluids in closed pipes. Values calculated by the model were compared to those obtained from the experimental rig of Holmboe and Rouleau (1967). The proposed model attained results with good agreement when compared to the experimental data. Frequencies, periods and amplitudes of oscillation were well represented for both water and oil (Newtonian fluids).

In sequence this model was compared to the one of Wahba (2013) by using a Non-Newtonian fluid that is governed by the Power Law equation. Once again the results showed excellent agreement. Next, an axial study of the evolution of the pressure head was conducted. It was observed that shear thickening fluids presented faster attenuations and that shear thinning fluids were less dissipative and they showed less variation of pressure head along the axial direction.

So this work has validated the proposed mathematical model with experimental and numerical data. It was also shown the importance of modelling the shear thickening and thinning behavior. Finally it can be concluded that this model is a great tool in order to better understand transient flows such as: the fluid hammer, the pressure transmission and the flow startup problems. Due to the new solution methodology that includes a constitutive equation; others Non Newtonian fluids may be easily changed and simulated.

7. ACKNOWLEDGEMENTS

The authors acknowledge the financial support of PETROBRAS S/A, ANP, FINEP, CNPq and CAPES.

8. REFERENCES

Anderson, J. D., 1990. *Modern compressible flow: with historical perspective*. McGraw Hill Higher Education.
Bird, R. B., Armstrong, R. C., and Hassager, O., 1987. *Dynamics of polymeric liquids. Vol. 1: Fluid mechanics*.
Davidson, M. R., Nguyen, Q. D., Chang, C., and Rønningsen, H. P., 2004. A model for restart of a pipeline with compressible gelled waxy crude oil. *Journal of non-newtonian fluid mechanics*, 123(2), 269-280.
Fortuna, A. O., 2000. *Técnicas computacionais para dinâminca dos fluidos: conceitos básicos e aplicações*. Edusp.
Holmboe, E. L., and Rouleau, W. T., 1967. The effect of viscous shear on transients in liquid lines. *Journal of Fluids Engineering*, 89(1), 174-180.
Negrão, C. O., Franco, A. T., and Rocha, L. L., 2011. A weakly compressible flow model for the restart of thixotropic drilling fluids. *Journal of Non-Newtonian Fluid Mechanics*, 166(23), 1369-1381.
Oliveira, G. M., da Rocha, L. L. V., Franco, A. T., and Negrão, C. O., 2010. Numerical simulation of the start-up of Bingham fluid flows in pipelines. *Journal of Non-Newtonian Fluid Mechanics*, 165(19), 1114-1128.
Oliveira, G. M., Negrão, C. O., and Franco, A. T., 2012. Pressure transmission in Bingham fluids compressed within a closed pipe. *Journal of Non-Newtonian Fluid Mechanics*, 169, 121-125.
Oliveira, G. M., Franco, A. T., Negrão, C. O., Martins, A. L., and Silva, R. A., 2013. Modeling and validation of pressure propagation in drilling fluids pumped into a closed well. *Journal of Petroleum Science and Engineering*, 103, 61-71.
Oliveira, G. M., Franco, A. T. and Negrão, C. O., 2015. Mathematical Model for Viscoplastic Fluid Hammer. *Journal of Fluids Engineering*.
Patankar, S., 1980. *Numerical heat transfer and fluid flow*. CRC Press.
Vinay, G., Wachs, A., and Agassant, J. F., 2006. Numerical simulation of weakly compressible Bingham flows: the restart of pipeline flows of waxy crude oils. *Journal of non-newtonian fluid mechanics*, 136(2), 93-105.
Vinay, G., Wachs, A., and Frigaard, I., 2007. Start-up transients and efficient computation of isothermal waxy crude oil flows. *Journal of non-newtonian fluid mechanics*, 143(2), 141-156.
Wachs, A., Vinay, G., and Frigaard, I., 2009. A 1.5 D numerical model for the start up of weakly compressible flow of a viscoplastic and thixotropic fluid in pipelines. *Journal of Non-Newtonian Fluid Mechanics*, 159(1), 81-94.
Wahba, E. M., 2008. Modelling the attenuation of laminar fluid transients in piping systems. *Applied Mathematical Modelling*, 32(12), 2863-2871.
Wahba, E. M., 2013. Non-Newtonian fluid hammer in elastic circular pipes: Shear-thinning and shear-thickening effects. *Journal of Non-Newtonian Fluid Mechanics*, 198, 24-30.
Watters, G. Z., 1984. *Analysis and control of unsteady flow in pipelines*. Boston: Butterworths.
White, F. M., 2003. *Fluid Mechanics*, WCB. ed: McGraw-Hill, Boston.
Wylie, E. B., Streeter, V. L., and Suo, L., 1993. *Fluid transients in systems* (Vol. 1, p. 464). Englewood Cliffs, NJ: Prentice Hall.

9. RESPONSIBILITY NOTICE

The authors are the only responsible for the printed material included in this paper.